VIŠEKRITERIJSKA OPTIMIZACIJA PROCESA TRAČNOG TESTERISANJA KOMADA PRSTENASTOG POPREČNOG PRESJEKA OD G-X55CRNISIS19-13-2 PRIMJENOM MOORA-TAGUCHI METODE

MULTICRITERIA OPTIMIZATION OF THE BAND SAWING PROCESS FOR RING-SHAPED CROSS-SECTION WORKPIECES MADE OF G-X55CRNISIS19-13-2 USING THE MOORA-TAGUCHI METHOD

***Edin Begović*[1]**
***Denis Bećirović*[2]**
***Adnan Mustafić*[2]**
***Sabahudin Ekinović*[1]**

[1]*University of Zenica Faculty of Mechanical Engineering, Fakultetska 1, Zenica, B&H*
[2]*University of Tuzla Faculty of Mechanical Engineering, Univerzitetska 4, Tuzla, B&H*

Stručni rad

REZIME:

Ovaj rad se fokusira na optimizaciju parametara procesa tračnog testerisanja debelostjenih cilindričnih komada od čelika G-X55CrNiSiS19-13-2. Primijenjena metodologija zasniva se na integrisanoj MOORA-Taguchi metodi, koja koristi Taguchi L16 ortogonalnu matricu sa tri kontrolisana faktora: brzina rezanja, brzina pomoćnog kretanja i dužine zahvata alata. Mjerljivi procesni parametri, posebno obrtni moment i snaga na pogonskom elektromotoru testere, kontinuirano su praćeni, dok su ostali pokazatelji indirektno određeni analitičkom metodom. Rezultati analize varijanse (ANOVA) pokazuju da svi ispitivani parametri značajno utiču na ukupnu performansu procesa, određenu primjenom MOORA metode.

Ključne riječi: *Tračno rezanje, Merec, Mora-Taguchi*
Keywords: Band sawing, Merec, Mora-Taguchi

Paper received: 04.04.2025.
Paper accepted: 26.09.2025.

Professional paper

ABSTRACT:

This paper focuses on the optimization of process parameters in band sawing of thick-walled cylindrical components made of G-X55CrNiSiS19-13-2 steel. The applied methodology is based on the integrated MOORA-Taguchi approach, utilizing the Taguchi L16 orthogonal array with three controlled factors: cutting speed, feed rate, and tool engagement length. Measurable process parameters, particularly torque and power on the saw drive motor, were continuously monitored, while other indicators were indirectly determined using analytical methods. The results of the analysis of variance (ANOVA) indicate that all examined parameters have a significant influence on the overall process performance, as determined by the application of the MOORA method.

1. INTRODUCTION

With the development and application of expensive and difficult-to-machine metals and metal alloys, minimizing waste in finishing operations has become increasingly important, along with the quality of the band sawing process [1]. The band sawing process is one of the fundamental methods used to prepare semi-finished products for further machining. It is primarily used for cutting semi-finished products to the required length, with attention given to the blade width. Sawing as a material machining method is inherently a rough process, with no variant of fine machining, aiming solely to divide semi-finished products at a specified length. Vertical band saws demonstrate efficiency and cost-effectiveness compared to other types of saws, especially when machining hard-to-cut materials and workpieces with larger cross-sections. Given the tools used in band sawing, which allow for narrow cuts with small cutting depths per tooth, only low driving power is required. These high-performance machines, characterized by high rigidity, compactness, and relatively simple construction, are most widely used in large-scale and mass metal processing production. The band sawing process involves a method that uses multi-tooth tools for fast separation of raw material. It is typically applied as the initial step in material removal processes and is crucial for mechanical machining. This technique is widely present in advanced industrial sectors, including aerospace, automotive, shipbuilding, and resource exploration [2]. A specific challenge in the sawing process is cutting high-alloy Cr-Ni steels. These hard-to-machine alloys possess specific mechanical properties that, besides having abrasive effects on the cutting tool, also cause significant tool load. The high content of alloying elements, especially Cr and Ni, promotes the formation of carbides and nitrides, which leads to abrasive wear and accelerated tool degradation. The formation of these compounds results in high temperatures in the cutting zone, complicating chip bending and breaking, leading to rapid tool wear and poor surface quality of the workpiece [3]. Authors Pengcheng Ni, Yangyu Wang, and others describe the problem of compound formation and their role in increasing the load during the sawing process. The increase in heat in the cutting zone also facilitates diffusion wear of the cutting tool, which reduces the tool's hardness and increases the hardness of the machined surface. This group of materials is also characterized by low thermal conductivity, meaning that most of the heat is carried away by the chips. This paper presents a method for selecting machining parameters based on a model of minimal effective cutting power consumption, minimal specific energy consumption, and minimal load on the cutting tool during the sawing of stainless steel. This model is essential for fully utilizing the performance of the sawing machine and improving machining efficiency.

2. EXPERIMENTAL SECTION

2.1. Machining System Configuration for Band Sawing

During the band sawing process on the vertical band saw type Kasto SSB A2, the workpiece remains stationary during cutting, and before the start of a new cycle, it is moved by a specified distance in a direction perpendicular to the tool (saw) movement. Given the specifics of the band sawing process, as well as the machine's characteristics, the main and auxiliary movements for this saw are driven by separate drives. Experimental tests of the sawing process were conducted at the CIMOS TMD Ai production facility in Gradačac, and included band sawing of small segments (~10 mm width) from a long workpiece. The tests were performed on a Kasto SSB A2 vertical band saw. This machine is robust, fully hydraulic, and designed for heavy-duty operations. Vertical band saws are known for their efficiency and cost-effectiveness, especially when machining hard-to-process materials and components with larger cross-sections. The saw blade speed is controlled via integrated technological tables, while the feed rate is manually adjusted using a continuous valve. During the cutting process, the hydraulic system is not engaged, ensuring a stable and continuous feed. Figure 1 shows the experimental setup for band sawing tests.

Figure 1 *Experimental Setup of the Band Sawing Process*

2.2. Measuring Equipment and Testing Procedure

By analysing the sawing process and considering the specific characteristics of the machine, such as separate drives for the main and auxiliary movements, cutting speed and feed rate were selected as control variables. For each cutting condition combination, a new cutting tool was installed. Following the recommendations of the saw and machine manufacturers, initial cuts were performed with lower parameter values to achieve the desired stability. At the beginning of each experimental combination, the feed rate and cutting speed were reduced to 50% of their nominal values. After 15 minutes of operating time or a total cutting area of approximately 300 cm², the cutting speed was increased to its nominal value, and the feed rate was then returned to its nominal value. A total of 200 samples were cut for each experimental combination, which approximately corresponds to standard production during one shift on a single machine. For every tenth sample cut, power, torque, voltage, and other electrical quantities were recorded using a mobile computer connected via an interface to the frequency converter and the corresponding software (FDS Tool). This procedure enabled the collection of raw data for subsequent offline analysis. The total power measured at the saw motor can be represented by the expression (1):

$$P_{tot} = P_{ef} + P_o \tag{1}$$

where P_{tot} represents the total measured power, P_{ef} represents the effective cutting power or the power required to perform the cutting process, and P_o represents the power consumed during idle operation, as shown in Figure 2.

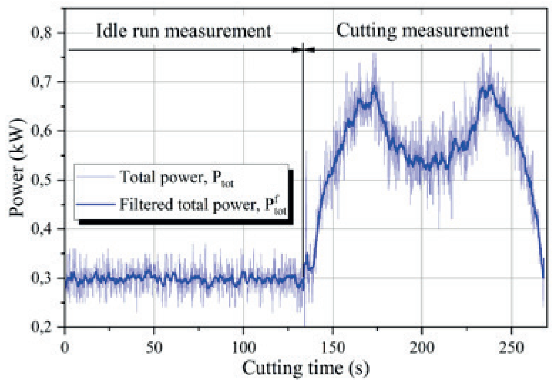

Figure 2 *Raw and filtered signals for total power and idle power during the band sawing process.*

As previously mentioned, specific cutting energy (E_{SP}) is a more efficient quantitative measure for assessing the cutting efficiency of metals or the machinability of the workpiece. It is calculated by dividing the effective power (P_{ef}) by the amount of material removed (MRR), as given in equation (2):

$$E_{SP} = \frac{P_{ef}}{MRR} \tag{2}$$

Cutting force is determined analytically through effective power and cutting speed, as given in equation (3):

$$P_{ef} = \frac{F_C \cdot v_c}{60 \cdot 10^3}\,[kW] \Rightarrow F_C = \frac{P_{ef}}{v_c} \cdot 60 \cdot 10^3 [N] \tag{3}$$

2.3. Workpiece Material and Cutting Tool Properties

In order to examine the impact of cutting parameters on the band saw load when machining high-alloy austenitic steel with a ring-shaped cross-section, a saw with carbide teeth of type Futura SN manufactured by WIKUS was used. This saw belongs to the group of saws with trapezoidal teeth and a variable tooth distribution, which are primarily used in the metal industry where high productivity is required when machining difficult-to-machine materials. Compared to other tooth shapes, trapezoidal teeth provide the best surface quality and are capable of cutting hardened steels with hardness up to 62 HRC, hard manganese steels, and chromium-nickel steels with diameters up to 250mm. The saw, which is in the form of an infinitely long band, is mounted on the drums of the machine tool and, rotating with the drums, performs discontinuous linear machining by sawing.

According to the manufacturer's specifications, the dimensions of the saw blade are L×W×H = 4115×41×1.3mm, with a variable tooth distribution of 3-4 teeth per inch. The workpiece used in the experiment was a cylindrical, thick-walled semi-finished product with dimensions Ø86×Ø38×505 mm. It was made of cast steel G-X55CrNiSiS19-13-2, which belongs to the category of stainless and heat-resistant steels. The chemical composition, appearance, and microstructure of the cast stainless steel are shown in Table 1. In this study of the band saw load, the material tested was cast steel type G-X55CrNiSiS19-13-2 (internal designation PL23), which belongs to the group of stainless and heat-resistant steels. The types of cast steels in this group are standardized according to DIN EN 10213-1. The chemical composition of this cast steel is within the limits shown in Table 1.

Table 1 Chemical Composition and Microstructure of the Material for Machining

G-X55CrNiSiS19-13-2		
Chemical composition	Min. [%]	Max. [%]
C	0,4	0,7
Si	1,8	2,20
Mn	---	1,5
S	0,20	0,40
P	---	0,06
Cr	18	21
Ni	12	14
Residuals	---	0,3
Fe	Balance	

Thick-walled cylindrical bars

Microstructure

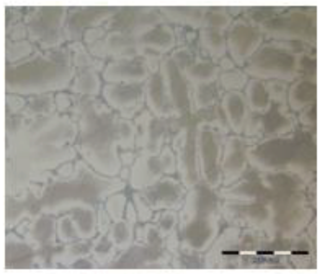

Centrifugal casting involves pouring molten steel into a rotating mold, where it solidifies under exceptionally high centrifugal forces, which can reach up to 120 times the gravitational acceleration. Due to the high rotational forces and the directional crystallization provided by the mold, a particularly clean and dense structure is formed. Impurities, inhomogeneities, and gas inclusions are pushed toward the surface layers due to their lower density compared to the steel, and these are later removed through mechanical processing of the semi-finished product. The semi-finished product, which has a ring-shaped cross-section, is cut to dimensions with an outer diameter of Ø85mm, an inner diameter of Ø38mm, and a total length of 505mm.

Due to differences in heat dissipation (viewed radially from the cross-section of the casting) and the influence of centrifugal forces on the semi-solidified and liquid metal, there is a difference in the grain size of the solidified structure. The grain size decreases from the inner diameter to the outer surface of the casting. This effect cannot be eliminated, but by adjusting the influencing parameters, this difference can be minimized.

As part of the research, metallographic preparation and microscopic imaging of the structure of the material being tested, as well as hardness testing, were performed in the laboratory complex of TMD Ai Gradačac. Figures 3 and 4 show the structure of the PL23 steel that was processed through band saw cutting.

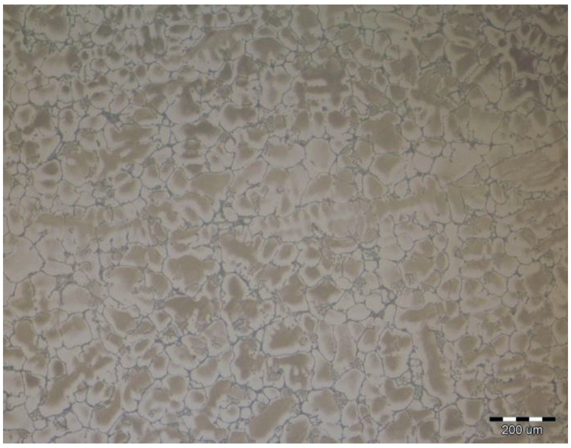

Figure 3 *Microstructure of cast stainless austenitic steel type G-X55CrNiSiS19-13-2*

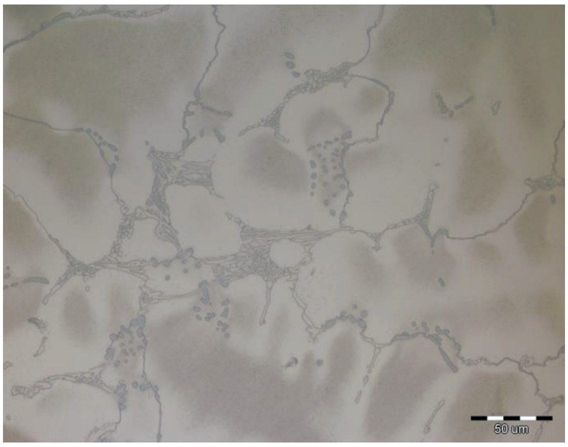

Figure 4 *An enlarged view of the microstructure showing a network of chromium carbides dispersed in the austenitic matrix*

Figure 5 shows the change in grain size of the structure, where it is clearly visible that observing from the inner diameter toward the outer one, there is a reduction in grain size. Due to differences in heat dissipation in the casting, an accompanying phenomenon of the grain structure change is also a variation in hardness for the tested material along the radial diameter.

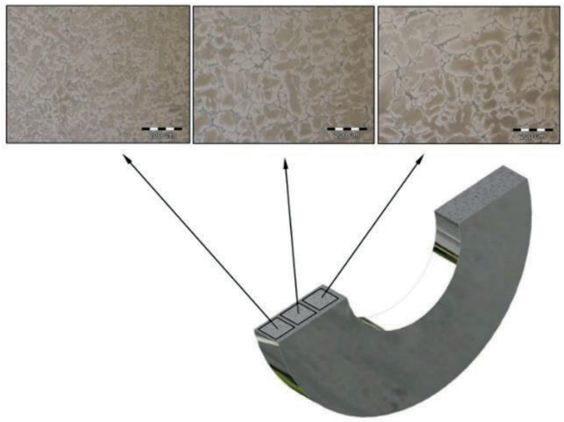

Figure 5 *Variation in grain size along the radial direction of the casting (thick-walled pipe)*

The structural changes that occur during the centrifugal casting method are also reflected in the hardness variation across the radial cross-section of the thick-walled pipe. Specifically, the hardness property depends on the grain size of the structure. A fine-grained material structure has higher hardness but lower toughness, while a coarse-grained structure has higher toughness but lower hardness. In this regard, by measuring the hardness across the radial cross-section of the ring, it should be found that the highest hardness, the hardest structure at the outer edge of the ring, while the lowest is at the inner edges.

2.4. Experimental Design

Considering the limitations of the experimental setup and the number of input parameters, the Taguchi method was selected for the experimental design. In this context, an L16 ($4^1 \times 2^2$) orthogonal array was used, in accordance with the principles of the Taguchi quality concept. The experimental design took into account the specific geometry of the workpiece, which had an annular cross-section. In addition to cutting speed and feed rate, the depth of cut was also included as one of the input parameters to ensure a comprehensive evaluation of the cutting process, as shown in Figure 6.

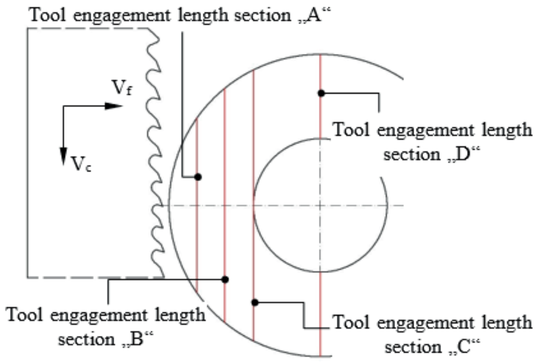

***Figure 6** Display of workpiece cross-section and tool engagement length*

Based on WIKUS's online calculator for defining relevant machining parameters in bandsaw cutting, depending on the type of machine tool used for the cutting operation, the bandsaw type, the material type, dimensions, shape of the workpiece, and the type of band sawing operation (standard cutting, cutting with increased tool life, or high-productivity cutting), the relevant machining parameters for the used bandsaw were adopted, as shown in Table 2.

Table 2 Experimental design settings

Symbol	Factors	Notation	Units	Level Values			
				1	2	3	4
A	Tool engagement length	TEL	(mm)	49 (**A**)	66 (**B**)	77 (**C**)	48 (**D**)
B	Cutting speed	Vc	(m/min)	40	52	-	-
C	Feed rate	Vf	(mm/min)	38	67	-	-

The experimentally measured values for each experimental run were repeated multiple times to ensure the required accuracy. The measured and calculated values of effective power, specific cutting energy, and total cutting force for three measurements according to the L16 experimental plan are shown in Table 3.

Table 3 Experimental run based on the L16 orthogonal array and measured responses.

Exp. run	A	B	C	P_{ef-1} (kW)	E_{sp_1} (J/cm^3)	F_1 (N)	P_{ef-2} (kW)	E_{sp_2} (J/cm^3)	F_2 (N)	P_{ef-3} (kW)	E_{sp_3} (J/cm^3)	F_3 (N)
1	1	1	1	0,19	450,29	289,97	0,19	445,11	286,63	0,18	416,64	268,30
2	1	1	2	0,21	374,37	308,92	0,23	414,77	342,25	0,24	436,98	360,59
3	1	2	1	0,21	376,27	241,85	0,23	408,19	262,37	0,24	424,15	272,62
4	1	2	2	0,25	327,61	283,72	0,26	340,94	295,26	0,24	319,81	276,96
5	2	1	1	0,30	696,16	448,30	0,31	724,63	466,63	0,32	753,10	484,97
6	2	1	2	0,34	618,76	510,59	0,38	683,40	563,92	0,35	634,92	523,92
7	2	2	1	0,32	577,73	371,34	0,36	645,55	414,93	0,40	719,35	462,37
8	2	2	2	0,46	617,77	535,00	0,45	600,01	519,62	0,44	582,64	504,58
9	3	1	1	0,35	825,57	531,63	0,37	866,98	558,30	0,36	832,04	535,80
10	3	1	2	0,42	766,21	632,25	0,43	786,40	648,92	0,44	804,58	663,92
11	3	2	1	0,45	811,10	521,34	0,49	876,93	563,65	0,42	761,24	489,29
12	3	2	2	0,54	722,88	626,03	0,51	685,87	593,98	0,51	676,39	585,77
13	4	1	1	0,23	526,32	338,92	0,25	584,55	376,42	0,23	540,87	348,30
14	4	1	2	0,28	505,66	417,25	0,26	471,32	388,92	0,25	463,24	382,25
15	4	2	1	0,26	468,03	300,83	0,30	529,86	340,57	0,30	539,83	346,98
16	4	2	2	0,31	416,44	360,64	0,33	446,04	386,28	0,35	472,54	409,23

2.5. Optimization Methodology

The Taguchi methodology uses S/N ratios to optimize process parameters by analysing response deviations from the target value in the presence of various noise conditions [4][5]. S/N ratios are applied to measure quality characteristics based on three criteria: smaller-is-better, nominal-is-best, and larger-is-better.

Since all responses need to be minimized, the smaller-is-better criterion is used, which can be applied using expression (4).

$$S/_{N} = -10\log\left(\frac{1}{n}\cdot\sum_{i=1}^{n} y_i^2\right) \qquad (4)$$

where y_i represents the response value obtained for experimental run i, and n represents the number of repeated experiments. Regardless of the quality characteristic, higher S/N ratio values indicate superior quality characteristics. Therefore, the optimal levels of process parameters are selected based on higher S/N ratio values [4][5]. The Taguchi signal-to-noise (S/N) ratios allow the identification of optimal levels for individual responses but not simultaneously. However, simultaneous optimization of process parameters is highly desirable in practical applications. Thus, in this study, after determining the S/N ratios for each response, the multi-objective optimization method based on ratio analysis (MOORA) was applied to achieve simultaneous response optimization. The steps followed for MOORA were adopted from Chakraborty's study [6], as follows:

Step 1: Create a decision matrix, denoted as *D*, of dimensions $m \times r$, where *m* represents the number of experimental runs and *r* represents the measured responses. The experimental runs contain different level combinations, as shown in Table 3. The values in decision matrix *D* are determined using expression (5).

$$D=\begin{bmatrix} \eta_{11} & \eta_{12} & \cdots & \eta_{1r} \\ \eta_{21} & \eta_{22} & \cdots & \eta_{2r} \\ \vdots & \vdots & \ddots & \vdots \\ \eta_{m1} & \eta_{m2} & \cdots & \eta_{mr} \end{bmatrix} \quad (5)$$

Step 2: Determination of the normalized decision matrix is determined using equation (6). The weighted normalized decision matrix (*V*) is calculated using equation (7). Weight of response *j* chosen by the decision maker is represented by w_j in equations $\sum_{j=1}^{r} w_j=1$:

$$\eta_{ij}^{*}=\frac{\eta_{ij}}{\sqrt{\sum_{i=1}^{m}(\eta_{ij})^2}},\; i=1,2,...,m;\; j=1,2,...,r; \quad (6)$$

$$V=\left[Y_{ij}\right]_{m\times r} \quad i=1,2,...,m \quad j=1,2,...,r; \quad (7)$$

$$Y_{ij}=\eta_{ij}^{*}\cdot w_j \quad (8)$$

where η_{ij}^{*} is a dimensionless number representing the normalized S/N ratio of scenario *i* on response *j*.

Step 3: Determination of MOORA performance index (Y_i^*) and ranking of alternatives is calculated using equation (9). For multi-objective optimization, weighted normalized values are added in case of maximization (for benefit response) and subtracted in case of minimization (for cost response) according to [7]:

$$Y_i^*=\sum_{j=1}^{t} Y_{ij} - \sum_{j=t+1}^{r} Y_{ij} \quad (9)$$

where the number of responses to be maximized is denoted by *t*, while the number of responses to be minimized is represented by (*r*-*t*). The ranking score of the *i*-th scenario with respect to all responses is denoted by (Y_i^*). A higher value of (Y_i^*) indicates better overall performance across multiple responses.

2.6. Method for Calculation of the Criterion Weight

The weight of the criteria in this study is determined by using the MEREC (Method based on the Removal Effects of Criteria) method. This method can be used by following the steps below [8][9].

Step 1: Set up the initial matrix as described in Step 1. of the MOORA method.

Step 2: Calculating the normalized values by:

$$h_{ij}=\frac{\min \lambda_{ij}}{\lambda_{ij}} \quad (10)$$

if the criterion *j* is as bigger as better, and

$$h_{ij}=\frac{\lambda_{ij}}{\max \lambda_{ij}} \quad (11)$$

if the criterion *j* is as smaller as better.

Step 3: Finding the alternative performance S_i by the following equation [8][9]:

$$S_i=\ln\left[1+\left(\frac{1}{n}\sum_j\left|\ln(h_{ij})\right|\right)\right] \quad (12)$$

Step 4: Estimating the performance of *i*th alternative S'_{ij} [8][9]:

$$S_i= \ln\left[1+\left(\frac{1}{k,k\neq j}\sum_j\left|\ln(h_{ij})\right|\right)\right] \quad (13)$$

Step 5: Finding the removal effect of the *j*th criterion E_j by:

$$E_j=\sum_i\left|S'_{ij}-S_i\right| \quad (14)$$

Step 6: Calculate the criterion weight by:

$$w_j=\frac{E_j}{\sum_k E_k} \quad (15)$$

3.0. RESULTS AND DISCUSSION

3.1. Individual Response Optimization Based on S/N Ratios

In the single response optimization approach, the basic idea is to minimize (or maximize) the mean value of the quality characteristic being investigated. In this work, the individual optimization of the responses was performed using signal-to-noise (S/N) ratios. For the effective cutting power, specific cutting energy, and total cutting force, the smaller-the-better quality characteristic based on S/N ratios was applied using equation (4). The results are tabulated in table 4. Larger values of S/N ratios indicate an excellent performance of responses.

Table 4 S/N ratios of individual responses

Experimental runs	A	B	C	*S/N P_{ef}*	*S/N E_{sp}*	*S/N F*
1	1	1	1	14,523	-52,821	-32,501
2	1	1	2	12,945	-52,246	-34,096
3	1	2	1	12,968	-52,114	-31,810
4	1	2	2	12,134	-50,359	-32,749
5	2	1	1	10,138	-57,207	-34,701
6	2	1	2	8,983	-56,208	-35,517
7	2	2	1	8,822	-56,260	-33,417
8	2	2	2	6,925	-55,568	-35,371
9	3	1	1	8,841	-58,503	-35,017
10	3	1	2	7,284	-57,907	-36,437
11	3	2	1	6,829	-58,253	-34,677
12	3	2	2	5,649	-56,844	-36,247
13	4	1	1	12,520	-54,825	-34,964
14	4	1	2	11,558	-53,632	-35,925
15	4	2	1	10,870	-54,212	-34,334
16	4	2	2	9,514	-52,979	-35,411

Higher S/N ratio values correspond to better responses, so based on the mean S/N ratios, the optimal parameters for individual responses were obtained. These are graphically presented in the main effects plots for S/N ratios in Figure 7.

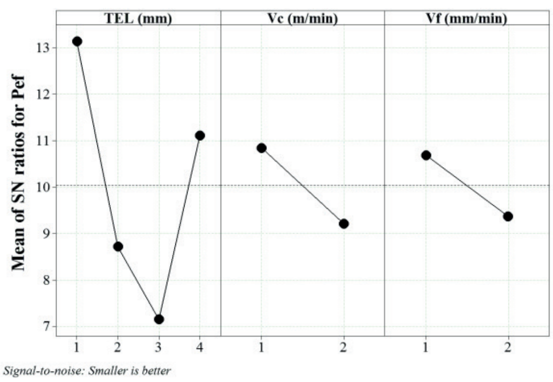

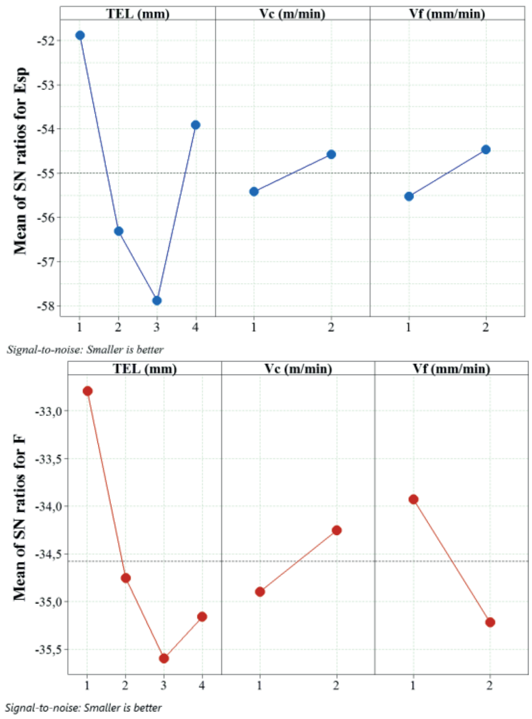

***Figure** 7 Main effects plots for S/N ratios (a) for effective cutting power Pef, (b) specific cutting energy Esp and (c) cutting force F*

Based on the presented results of experimentally measured and calculated quantities, it is evident that the tool engagement length (TEL) shows consistent variations across all output characteristics. Specifically, the highest values of power, specific cutting energy, and cutting force were recorded at the third level, which corresponds to the maximum depth of cut on the workpiece. However, cutting speed and feed rate do not have a unique parameter combination that satisfies all experimentally measured responses. Consequently, a multi-criteria optimization analysis is necessary to overcome these limitations. This approach involves creating a joint quality characteristic that optimizes all output responses simultaneously.

4.0. MULTI-CRITERIA OPTIMIZATION USING THE MOORA METHOD

The optimization of process parameters was performed for the S/N ratios of individual responses shown in Table 4. The analysis of S/N ratios enables better quantification of the influence of individual factors on system responses, with a particular focus on reducing noise in the data. Additionally, by applying S/N ratios within the MOORA method, the analysis becomes less sensitive to variations in experimental conditions, thereby increasing the statistical significance of the results. This approach ensures that the optimization is not subject to deviations that may arise due to measurement uncertainty or minor changes in experimental setups. The optimization methodology is described in Section 2.5. The overall analysis encompasses the influence of variation in three process parameters on three different responses of the metal machining system. To perform the optimization, it was necessary to determine the weighting factors of the system's output values to avoid subjective opinions of the author. For this purpose, the MEREC method, described in Section 2.6, was applied. The MEREC methodology yielded the following criterion weight values for parameter influence:

Table 5 The criterion weight values according to the MEREC method

	Criterion weight values		
wj	Pef (W)	Fz (N)	SCE (J/cm3)
	0,456117	0,186786	0,3570976

According to Table 5, the highest weighting factor belongs to effective cutting power, followed by specific cutting energy, and finally cutting force. After calculating the influence weight values, a performance index was computed to consolidate all output vector values (measured and calculated quantities) into a single performance measure. The calculated performance index values Y_i are presented in Table 6.

Table 6 Optimization of process parameters using the MOORA methodology

R.br.	S/N ratio			Normalized matrix			Weighted matrix			Performance index Yi	Rank
	Pef	Fz	Esp	Pef	Fz	Esp	Pef	Fz	Esp		
1	**14.52322**	**-32.5005**	**-52.8215**	**0.351012**	**-0.23484**	**-0.23989**	**0.160102**	**-0.04387**	**-0.08566**	**0.030574124**	**1**
2	12.945253	-34.0955	-52.24565	0.3128738	-0.246367	-0.237272	0.142707	-0.046018	-0.084729	0.011959903	3
3	12.96819	-31.80992	-52.11388	0.3134282	-0.229852	-0.236674	0.1429599	-0.042933	-0.084516	0.015511262	2
4	12.133503	-32.74939	-50.35889	0.2932546	-0.236641	-0.228703	0.1337584	-0.044201	-0.081669	0.007887925	4
5	10.137871	-34.70066	-57.20685	0.2450222	-0.25074	-0.259803	0.1117588	-0.046835	-0.092775	-0.027850931	8
6	8.9825353	-35.51652	-56.20837	0.2170989	-0.256635	-0.255269	0.0990225	-0.047936	-0.091156	-0.040069095	11
7	8.8221855	-33.4172	-56.25988	0.2132234	-0.241466	-0.255503	0.0972548	-0.045102	-0.091239	-0.039086918	10
8	6.9248654	-35.37148	-55.56753	0.1673671	-0.255587	-0.252358	0.0763389	-0.04774	-0.090117	-0.061517575	13
9	8.8412597	-35.01697	-58.50346	0.2136844	-0.253026	-0.265692	0.0974651	-0.047262	-0.094878	-0.044674333	12
10	7.2837046	-36.43673	-57.9072	0.1760399	-0.263284	-0.262984	0.0802947	-0.049178	-0.093911	-0.062793879	14
11	6.8291768	-34.67744	-58.25289	0.1650544	-0.250572	-0.264554	0.0752841	-0.046803	-0.094472	-0.065990687	15
12	5.6485013	-36.24692	-56.84389	0.1365186	-0.261913	-0.258155	0.0622684	-0.048922	-0.092186	-0.078839568	16
13	12.519549	-34.96424	-54.82517	0.302585	-0.252645	-0.248987	0.1380141	-0.04719	-0.088913	0.001911142	5
14	11.558421	-35.92494	-53.63248	0.2793555	-0.259586	-0.24357	0.1274187	-0.048487	-0.086978	-0.008046616	6
15	10.870294	-34.33394	-54.21177	0.2627241	-0.24809	-0.246201	0.1198329	-0.04634	-0.087918	-0.014424584	7
16	9.5135333	-35.41084	-52.97886	0.2299326	-0.255872	-0.240602	0.1048761	-0.047793	-0.085918	-0.028835346	9

The highest performance index value will determine the optimum for the given machining process. In this case, the optimal process parameter values are achieved with the parameters from the first point of the experimental array. This experimental point has input parameter values in coded form as A1-B1-C1, which correspond to natural values of TEL=49 mm, v_c=40 m/min i v_f=38 mm/min. To confirm the optimization of process parameters, statistical data processing was performed using ANOVA within a defined significance threshold of 5% (p≤0.05). The analysis of variance for the performance index Y_i revealed that all three process parameters have a significant influence on the system response. According to Table 7, the most significant influence comes from the depth of cut, followed by cutting speed, and then feed rate. The coefficient of determination for the performance index is quite high, with a value of 0.99.

Table 7 Analysis of variance of the performance index Y_i

Source	DF	Seq SS	Contribution	Adj SS	Adj MS	F-Value	P-Value
TEL (mm)	3	0,014495	87,98%	0,014495	0,004832	346,46	0,0000
v_C (m/min)	1	0,000997	6,05%	0,000997	0,000997	71,5	0,0000
v_f (mm/min)	1	0,000844	5,12%	0,000844	0,000844	60,54	0,0000
Error	10	0,000139	0,85%	0,000139	0,000014		
Total	15	0,016476	100,00%				

Based on this coefficient, it can be concluded that 99.15% of the variability in the dependent variable Yi is attributed to the influence of the process parameters. By analysing the mean effects of the process parameters on the performance index, according to the "larger is better" criterion, the optimization model is confirmed. Higher values of the signal-to-noise ratio in the main effects plot correspond to a better response. Based on the diagram in the following figure, it is clear that the influence of the tool engagement length is the most significant on the performance index and has a curvilinear effect on the response. The other two parameters have a linear influence on the performance index, and their impact is approximately equally significant.

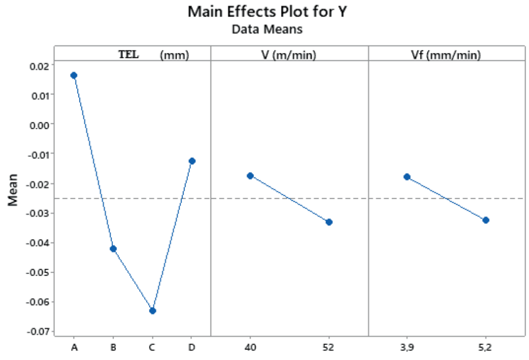

Figure 8 *The main effects plot for the "larger is better" criterion regarding the performance index*

The main effects plot for the performance index, according to the "larger is better" criterion, shows that the machining system for sawing will achieve optimal performance at the coded parameter values A1-B1-C1, which correspond to the actual values of TEL=49 mm, v_c=40 m/min i v_f=38 mm/min.

5. CONCLUSIONS

This study employed the multi-criteria optimization method MOORA-Taguchi. Three output parameters were observed: effective cutting power, specific cutting energy, and cutting force, while the selected process parameters were tool engagement length, cutting speed, and feed rate. In this context, the tool engagement length was varied at four levels, while the other two process parameters were varied at two levels in accordance with the manufacturer's recommendations. The Taguchi experimental design in this case prescribed an L_{16} ($4^1 \times 2^2$) orthogonal array. Each experimental run was repeated three times. The machining system used for the experiments was a Kasto SSB A2 vertical bandsaw machine, and data acquisition was performed using FDS Tool software.

Following statistical analysis and the calculation of performance measures for each parameter, the results were evaluated based on the *"smaller is better"* criterion. The obtained results provided suboptimal solutions, necessitating the application of multi-criteria analysis. In this regard, weighting factors were calculated using the MEREC method, followed by optimization using the MOORA method. Based on the findings, the following conclusions can be drawn:

- Graphical interpretation of the influence of machining parameters on effective cutting power reveals the process parameter values that minimize effective cutting power. According to Figure 4, the minimum value of specific cutting power is achieved at a tool engagement length of 49 mm, cutting speed of 40 m/min, and feed rate of 38 mm/min.
- Graphical interpretation of the influence of machining parameters on specific cutting energy indicates the process parameter values that minimize specific cutting energy. As shown in Figure 4, the minimum value of specific cutting power is achieved at a tool engagement length of 49 mm, cutting speed of 52 m/min, and feed rate of 67 mm/min.
- Graphical interpretation of the influence of machining parameters on cutting force demonstrates the process parameter values that minimize cutting force. Based on Figure 4, the minimum value of specific cutting power is obtained at a tool engagement length of 49 mm, cutting speed of 52 m/min, and feed rate of 38 mm/min.
- The calculation of weighting factors using the MEREC method ensures a methodological and objective decision-making process, eliminating author bias. The highest weighting factor was assigned to P_{ef} (0.4561), followed by F_Z (0.3570), and finally E_{sp} (0.1867).
- Based on the conducted optimization, the minimum values of the output parameters were achieved with the following combination: TEL=49 mm, v_c= 40 m/min, and v_f = 38 mm/min.
- Analysis of variance (ANOVA) of the performance index confirmed that all three process parameters have a significant influence on the system response, with a coefficient of determination (R^2) of 99.15%.
- The main effects plot for the performance index Yi validated the nature of the influence of process parameters and the experimental parameter combination obtained through the MOORA optimization method, corresponding to the actual values of TEL=49 mm, v_c= 40 m/min, and v_f= 38 mm/min.

6. REFERENCES

[1] Primož Potočnik, Tilen Thalerb, Edvard Govekar: „Multisensory chatter detection in band sawing“ (2013.), 14th CIRP Conference on Modeling of Machining Operations (CIRP CMMO), CIRP 8 (2013) 469 – 474.

[2] Bing Chen, Wenzhang Yang, Zihao Liu: „A fuzzy control based strategy for adjusting band blade feed rate in constant power sawing“ (2024.), Measurement Science and Technology,Vol. 6 (2025) 015603 (15pp).

[3] A. I. Fernández-Abia, J. Barreiro, L. N. López de Lacalle, S. Martínez: „Research on optimization method of stainless steel sawing process parameters based on multi-tooth sawing force prediction model“ (2012.), The International Journal of Advanced Manufacturing Technology, DOI 10.1007/s00170-011-3267-9.

[4] Gauri, Susanta Kumar Chakraborty, Shankar: „Multi-response optimisation of WEDM process using principal component analysis, International Journal of Advanced Manufacturing Technology“, Vol. 41, Issue 7-8, 2009.

[5] Abas, Muhammad Sayd, Lal Akhtar, Rehman Khalid, Qazi Salman Khan, Aqib Mashood Pruncu, Catalin Iulian: „Optimization of machining parameters of aluminum alloy 6026-T9 under MQL-assisted turning process“, Journal of Materials Research and Technology, Vol. 9, Issue 5., 2020.

[6] Chakraborty, Shankar: „Applications of the MOORA method for decision making in manufacturing environment“, International Journal of Advanced Manufacturing Technology, Vol. 54, Issue 9-12, 2011.

[7] Tansel, Yusuf Iç Yldrm, Sebla: „MOORA-based Taguchi optimisation for improving product or process quality“, International Journal of Production Research, Vol. 51, Issue 11, 2013.

[8] Abas, Muhammad Habib, Tufail Noor, Sahar Salah, Bashir Zimon, Dominik: „Parametric Investigation and Optimization to Study the Effect of Process Parameters on the Dimensional Deviation of Fused Deposition Modeling of 3D Printed Parts“, PolymersVol.14, Issue 17., 2022.

[9] Le, Hoang Anh, Hoang, Xuan Tu,Trieu, Quy Huy Pham, Duc Lam Le, Xuan Hung: „Determining the Best Dressing Parameters for External Cylindrical Grinding Using MABAC Method“, Applied Sciences, Vol. 12. Issue 16, 2022

Corresponding author:
Denis Bećirović
University of Tuzla
Faculty of Mechanical Engineering,
Univerzitetska 4, Tuzla, B&H
Email: untz.denis.becirovic@gmail.com